

1 **Non-apoptotic pioneer neutrophils initiate an endogenous swarming response in a**  
2 **zebrafish tissue injury model**

3 Hannah M. Isles<sup>1,2</sup>, Clare F. Muir<sup>1,2</sup>, Noémie Hamilton<sup>1,2</sup>, Anastasia Kadochnikova<sup>3</sup>, Catherine  
4 A. Loynes<sup>1,2</sup>, Visakan Kadiramanathan<sup>3</sup>, Philip M. Elks<sup>1,2\*</sup>, Stephen A. Renshaw<sup>1,2\*,\*\*</sup>

5 <sup>1</sup> The Bateson Centre, University of Sheffield, Firth Court, Western Bank, Sheffield S10 2TN,  
6 UK.

7 <sup>2</sup> Department of Infection, Immunity and Cardiovascular Disease, University of Sheffield  
8 Medical School, Beech Hill Road, Sheffield S10 2RX, UK.

9 <sup>3</sup> Department of Automatic Control and Systems Engineering, University of Sheffield, Mappin  
10 Street, Sheffield, S1 3JD, UK.

11 \*joint senior authors

12

13

14

15

16

17 **\*\*Corresponding Author:** Stephen A. Renshaw ([s.a.renshaw@sheffield.ac.uk](mailto:s.a.renshaw@sheffield.ac.uk))

18

19

20

21

22

23

24

25 **Abstract**

26 Neutrophils are rapidly recruited to inflammatory sites where they are able to coordinate their  
27 migration to form clusters, a process termed neutrophil swarming. The factors which initiate  
28 neutrophil swarming are not understood, requiring the development of new *in vivo* models.  
29 Using transgenic zebrafish larvae to study neutrophil migration, we demonstrate that  
30 neutrophil swarming is conserved in zebrafish immunity, sharing essential features with  
31 mammalian systems. We identified that one pioneer neutrophil was sufficient to induce  
32 neutrophil swarming after adopting a distinctive morphology at the wound site, followed by the  
33 coordinated migration of neutrophils to form a swarm. Using a FRET reporter of neutrophil  
34 apoptosis, we demonstrate that pioneer neutrophils do not undergo caspase-3 mediated  
35 apoptosis prior to swarming. These data provide some of the first evidence of endogenous  
36 neutrophil migration patterns prior to swarming and demonstrate that the zebrafish can be  
37 used to dissect the mechanisms modulating neutrophil swarm initiation.

38

## 39 Introduction

40 Inflammation is the coordinated response of immune cells to invading pathogens or  
41 endogenous danger signals. Sterile inflammation has evolved as a physiological response to  
42 noxious stimuli including mechanical trauma, ischemia, toxins and antigens in the absence of  
43 infection<sup>1</sup>. Neutrophils are one of the first responders to sterile inflammation, which rapidly  
44 home to inflamed tissue within hours of injury. Within inflamed tissue, neutrophils carry out  
45 specialised functions to destroy pathogens<sup>2</sup> and repair damage<sup>3</sup>, ultimately leading to the  
46 restoration of tissue homeostasis. Neutrophils are recruited to an inflammatory stimulus  
47 through a series of well-defined molecular events which lead to their extravasation from the  
48 circulation into the tissue<sup>4-6</sup>. During their recruitment, neutrophils are primed by pro-  
49 inflammatory stimuli including growth factors, inflammatory cytokines and chemoattractants,  
50 a process which increases responsiveness to activating agents and enhances neutrophil  
51 function<sup>7</sup>. Within interstitial tissues, neutrophils are capable of integrating host- and pathogen-  
52 derived environmental signals, resulting in their polarisation and migration towards the  
53 initiating inflammatory stimulus<sup>8</sup>. However, the precise mechanisms by which neutrophils  
54 coordinate their migration and function within the complexity of inflamed interstitial tissue  
55 remain to be understood.

56 Advances in intravital imaging have increased our understanding of the spatiotemporal  
57 dynamics of neutrophil migration within interstitial tissue *in vivo*<sup>9</sup>. Neutrophils in the interstitium  
58 coordinate their migration patterns to form clusters in several models of sterile-inflammation  
59 and infection<sup>9-13</sup>. The parallels between these cellular behaviours and migration patterns seen  
60 in insects has led to use of the term “swarming”. A series of sequential phases leading to  
61 neutrophil swarming have been described; the initial migration of ‘pioneer’ or ‘scouting’  
62 neutrophils proximal to the wound site (scouting) is followed by large scale synchronised  
63 migration of neutrophils from distant regions (amplification) leading to neutrophil clustering  
64 (stabilisation) and eventually resolution<sup>9-12</sup>. Communication between neutrophils during  
65 swarming is complex. Many chemoattractants including lipid and proteins mediate the  
66 response, with a dominant role for the lipid leukotriene B4 (LTB4) identified *in vivo*<sup>10,11</sup>. LTB4  
67 produced by early responding neutrophils amplifies neutrophil tissue responses by signal relay  
68 to more distant tissue regions<sup>11,14</sup>. Less is understood about the initiating signals required for  
69 neutrophil attraction during the early stages of neutrophil swarming at sites of tissue damage.

70 Various chemoattractants from damaged cells and pathogens are present within an inflamed  
71 tissue during the early stages of inflammation, making the functional dissection of the signals  
72 required for neutrophil swarming challenging. The initial arrest and clustering of a small

73 number of early-recruited pioneer neutrophils precedes large scale migration of other  
74 neutrophils, leading to cluster growth<sup>9,11</sup>. In the context of tissue injury, cell death within the  
75 initial neutrophil cluster has been found to correlate with an amplification of neutrophil  
76 recruitment<sup>11</sup> and, in the context of infection, lysis of infected cells followed by parasite egress  
77 is associated with swarm formation<sup>12</sup>. Based on these migration patterns, it is likely that  
78 swarming neutrophils respond to an amplified signal initiated by pioneer neutrophils. The  
79 release of death signals including extracellular NAD<sup>+</sup> from dying pioneer neutrophils has been  
80 implicated in swarm initiation<sup>9</sup>, although the precise nature of these signals remains to be  
81 determined.

82 New models are required to study the migration patterns of endogenous neutrophils *in vivo*  
83 during early swarm formation to understand the precise signalling and tissue context required  
84 for swarm initiation. The zebrafish (*Danio rerio*) is a powerful model organism in which to study  
85 neutrophil function that is used extensively to study neutrophil migration towards and away  
86 from sites of sterile inflammation<sup>15–17</sup>. The optical transparency of transgenic zebrafish  
87 embryos allows for the tracking of endogenous GFP labelled neutrophils to wound sites within  
88 minutes following injury<sup>18</sup>. In this study, we use both inflammation and infection assays to  
89 demonstrate that neutrophil swarming is conserved in zebrafish immunity, highlighting the  
90 importance of this neutrophil behaviour across evolution. We define a three-stage sequence  
91 of migration events which leads to the swarming of endogenous neutrophils within the inflamed  
92 tissue and verify that LTB<sub>4</sub> signalling is required for amplification of neutrophil recruitment.  
93 Importantly, we show that a single pioneer neutrophil is sufficient to induce a swarming  
94 response in a significant proportion of larvae and that this neutrophil adopts a phenotype  
95 distinct from other neutrophils within the inflamed tissue. We study neutrophil swarm initiation  
96 in a transgenic reporter of neutrophil apoptosis, and confirm that swarm initiating pioneer  
97 neutrophils are not apoptotic. Finally, we have identified that endogenous pioneer neutrophils  
98 can be imaged *in situ* prior to the swarming response, making the zebrafish an excellent model  
99 to dissect the signalling pathways which mediate swarm initiation.

100

101

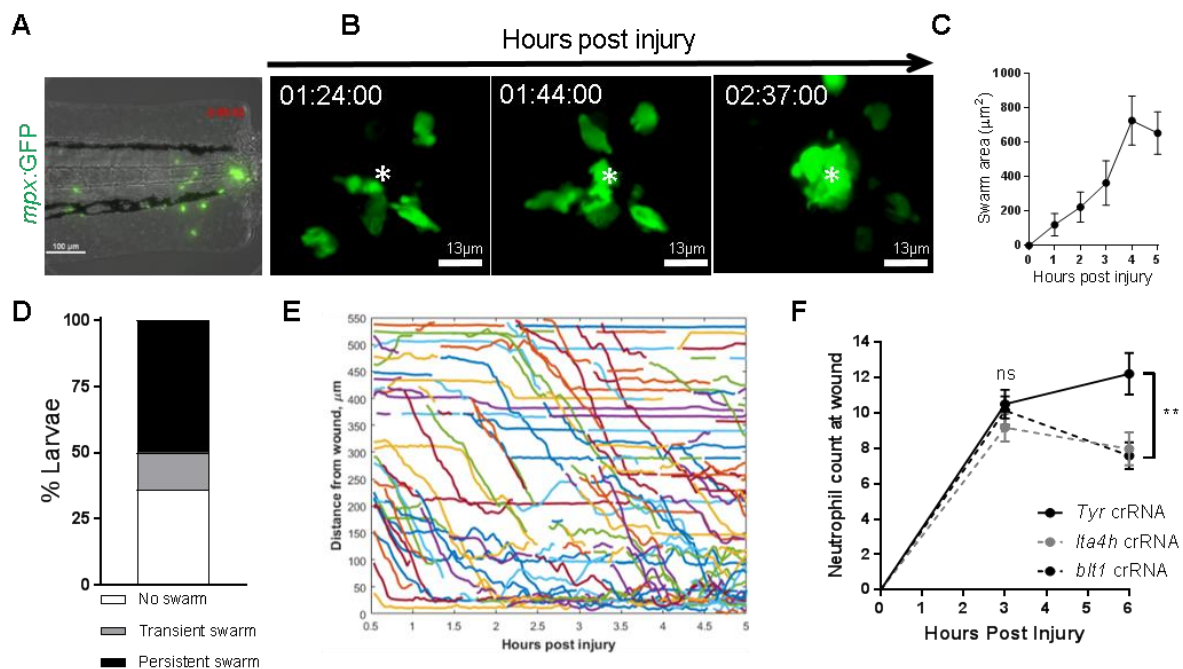
## 102 Results

### 103 Neutrophil swarming is conserved in the zebrafish tissue damage response

104 Neutrophil swarming is characterised by the highly directed and coordinated movement of  
105 neutrophils followed by accumulation and clustering at sites of infection or injury<sup>19</sup>. To  
106 determine whether neutrophil swarming is conserved in zebrafish immunity we studied  
107 neutrophil mobilisation to inflammatory and infectious stimuli. Neutrophil responses to  
108 inflammatory stimuli were assessed by transecting the tail-fins of 3 days post fertilisation (dpf)  
109 *mpx:GFP* larvae, and tracking neutrophil migration using fluorescence microscopy during the  
110 recruitment phase (0-6 hours post injury, Supplementary Figure 1 and as previously  
111 described<sup>18</sup>). Analysis of migration patterns of neutrophils recruited to the wound site identified  
112 three outcomes: 1) persistent neutrophil swarming reminiscent of neutrophil swarming  
113 reported in mammalian systems<sup>9-12</sup> (Figure 1A-C, Supplemental Movie 1); 2) shorter lived  
114 transient neutrophil swarms which dissipated and reformed multiple times within the imaging  
115 period (Supplemental Figure 2, Supplemental Movie 2); 3) no coordinated migration leading  
116 to swarm formation (Supplemental Movie 3). Persistent swarming was defined as the  
117 formation of clusters which grew throughout the imaging period by the coordinated migration  
118 of individual neutrophils (Figure 1C). Persistent swarms were observed from 40 minutes post  
119 injury (Supplemental Figure 3A) and remained stable for 2.17 hours  $\pm$  0.32 (Supplemental  
120 Figure 3B). In our imaging experiments (n=14 larvae from 5 experimental repeats), persistent  
121 neutrophil swarms were observed in 50% of larvae, transient swarms (persisting for <1 hour)  
122 were seen in 14% of larvae, and no evidence of swarming behaviour within the imaging period  
123 in 36% of larvae (Figure 1D). During the imaging period, two stages of neutrophil recruitment  
124 were observed: the early migration of neutrophils proximal to the wound site (approximately  
125 closer than 350 $\mu$ m) within minutes following injury, followed by an influx of neutrophils from  
126 more distant sites (approximately further than 350 $\mu$ m) from around 60 minutes post injury  
127 (Figure 1E).

128 In mammalian neutrophil swarming biphasic neutrophil responses are modulated by the lipid  
129 LTB<sub>4</sub><sup>11</sup>. We investigated the requirement for LTB<sub>4</sub> in neutrophil chemotaxis towards the  
130 wound site in zebrafish using the CRISPR/Cas9 system. Biosynthesis of LTB<sub>4</sub> in zebrafish  
131 occurs through fatty acid metabolism of arachidonic acid via common intermediates, resulting  
132 in the production of LTB<sub>4</sub> by the enzyme leukotriene A<sub>4</sub> hydrolase (LTA<sub>4</sub>H), encoded by the  
133 gene *Ita4h*<sup>20,21</sup>. Zebrafish have three LTB<sub>4</sub> receptors; the high affinity *blt1* receptor and two  
134 low affinity receptors *blt2a* and *blt2b*, of which neutrophils predominantly express *blt1*  
135 (Supplemental Figure 4A-B). Using Cas9 protein with guide RNAs (crRNAs) to target *Ita4h*  
136 and *blt1*, early neutrophil recruitment (3hpi) and late neutrophil (6hpi) responses to the wound

137 site were assessed. A crRNA targeting the pigment gene tyrosinase (*tyr*)<sup>22</sup> was used for control  
 138 injections and to allow for visual identification of successful knockdown. Knockdown of *tyr*  
 139 produces an albino phenotype in zebrafish larvae (Supplemental Figure 5A) without affecting  
 140 neutrophil development or the neutrophilic inflammatory response (Supplemental Figure 5B-  
 141 C). Early neutrophil recruitment to the wound site at 3hpi was similar between control (*tyr*),  
 142 *blt1* and *lta4h* crRNA injected larvae (Figure 1F), suggesting that LTB4 signalling is not  
 143 required for early neutrophil responses. Interestingly at 6hpi, neutrophil recruitment in control  
 144 (*tyr*) crRNA injected larvae increased as anticipated (Supplemental Figure 1), however, this  
 145 increase in recruitment was not seen in *blt1* and *lta4h* crRNA injected larvae, which displayed  
 146 significantly lower neutrophil counts at 6hpi compared to control larvae (Figure 1F). These  
 147 results are in agreement with data from mouse<sup>11</sup> and human neutrophils<sup>10</sup>, supporting a role  
 148 for LTB4 signalling in neutrophil recruitment at the later stages.



149

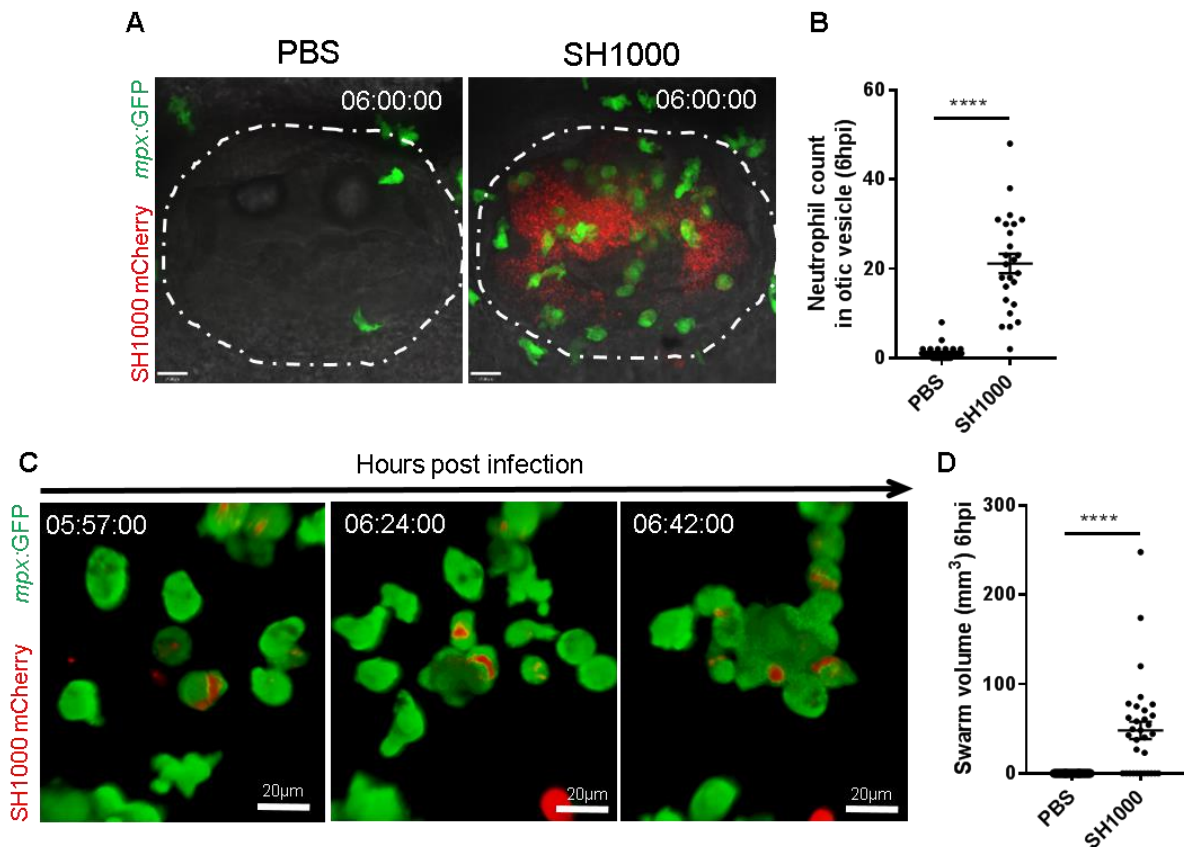
150 **Figure 1. Neutrophil swarming is conserved in the zebrafish tissue damage response**

151 **A-C.** Zebrafish neutrophils swarm at sites of tissue damage. **A.** Representative example (from  
 152 5 experimental repeats) of neutrophils swarming at the wound site following tail fin transection  
 153 in 3dpf *mpx:GFP* larvae. Bright field highlights tail fin region. Time stamp shown is relative to  
 154 the start of the imaging period at 30 minutes post injury and is h:mm:ss. **B.** 3D reconstruction  
 155 time course illustrating neutrophils swarming at the wound site, where the swarm centre is  
 156 highlighted by an asterisk. Imaging was performed using a 40X objective spinning disk confocal  
 157 microscope. Time stamps shown are relative to time post injury and are in hh:mm:ss. **C.** Area

158 of neutrophil swarms measured at the wound site during the 5 hour imaging period. Error bars  
159 shown are mean  $\pm$  SEM, n=5 experimental repeats. **D.** Proportion of neutrophil swarming  
160 behaviour observed at the wound site within 5 hours following injury, n=5 experimental  
161 repeats. **E-F.** Relay signalling through LTB4 is required for neutrophil recruitment. **E.**  
162 Distance/time plot demonstrating the early recruitment of neutrophils proximal to the wound  
163 site (<350 $\mu$ m) followed by the later recruitment of more distant neutrophils. **F.** CRISPR/Cas9-  
164 mediated knockdown of LTB4 signalling reduces late neutrophil recruitment. Neutrophil counts  
165 at the wound site in control *tyr* crRNA injected larvae (black line), *Ita4h* crRNA injected larvae  
166 (grey dotted line), and *blt1* crRNA injected larvae (black dotted line) at 3 and 6hpi. Error bars  
167 shown are mean  $\pm$  SEM. Groups were analysed using an ordinary one-way ANOVA and  
168 adjusted using Tukey's multi comparison test. \*\*p>0.008 n=45 from 3 independent  
169 experiments.

## 170 **Neutrophil swarming is conserved in the zebrafish response to infection**

171 After determining that swarming was a conserved component of the tissue damage response  
172 in zebrafish, neutrophil responses to infectious stimuli were assessed. *Staphylococcus*  
173 *aureus*, a gram positive bacteria which induces a neutrophil swarming response in mammalian  
174 neutrophils<sup>23</sup>, was injected into the left otic vesicle of 2dpf *mpx*:GFP larvae. Injection of *S.*  
175 *aureus* induced robust neutrophil recruitment (21 $\pm$ 2 neutrophils) to the otic vesicle at 6 hours  
176 post injury, which was not seen in larvae injected with a PBS control (1 $\pm$ 0.3 neutrophils)  
177 (Figure 2A-B). To observe the migration patterns of zebrafish neutrophils in real time within  
178 infected otic vesicles, time-lapse imaging of neutrophil mobilisation towards *S. aureus*  
179 infection was performed from 1-hour post infection for 6 hours (Figure 2C). Neutrophils within  
180 otic vesicles infected with *S. aureus*, but not PBS, coordinated their migration to form swarms  
181 in tissue regions containing bacteria, which at 6hpi had an average volume of 48.1mm<sup>3</sup> (Figure  
182 2D, Supplemental Movie 4). The identification of neutrophil swarming in response to  
183 inflammatory and infectious stimuli demonstrates that neutrophil swarming is a conserved  
184 component of zebrafish immunity. We therefore used the zebrafish model to study the early  
185 migration patterns of neutrophils prior to the swarming response.



186

187 **Figure 2. Zebrafish neutrophils swarm to *S. aureus* infection**

188 **A.** Otic vesicles of 2dpf *mpX:GFP* larvae injected with a PBS vehicle control or 2500 cfu *S.*  
189 *aureus* SH1000 pMV158mCherry. Otic vesicles are highlighted by white dashed area. Time  
190 stamps shown are hh:mm relative to time post infection. **B.** Neutrophils mobilised to the otic  
191 vesicle at 6hpi. Error bars shown are mean  $\pm$  SEM (n=32 larvae from 3 independent  
192 experiments). Error bars shown are mean  $\pm$  SEM \*\*\*\*p>0.0001 from an un-paired t-test, n=32  
193 from 3 independent repeats. **C-E.** Zebrafish neutrophils swarm at *S. aureus* infection. **C.** 3D  
194 reconstruction time course illustrating neutrophil swarming within otic vesicle of 2dpf *mpX:GFP*  
195 larvae injected with 2500 cfu *S. aureus* SH1000 pMV158mCherry. Imaging was performed  
196 using a 20X objective spinning disk confocal microscope. Time stamps shown are hh:mm:ss  
197 relative to time post injection. **D.** Volume of neutrophil swarms measured within otic vesicle at  
198 6hpi. A volume of zero corresponds to no swarm observed. Error bars shown are mean  $\pm$  SEM  
199 \*\*\*\*p>0.0001 from an un-paired t-test, n=32 from 3 independent experiments.

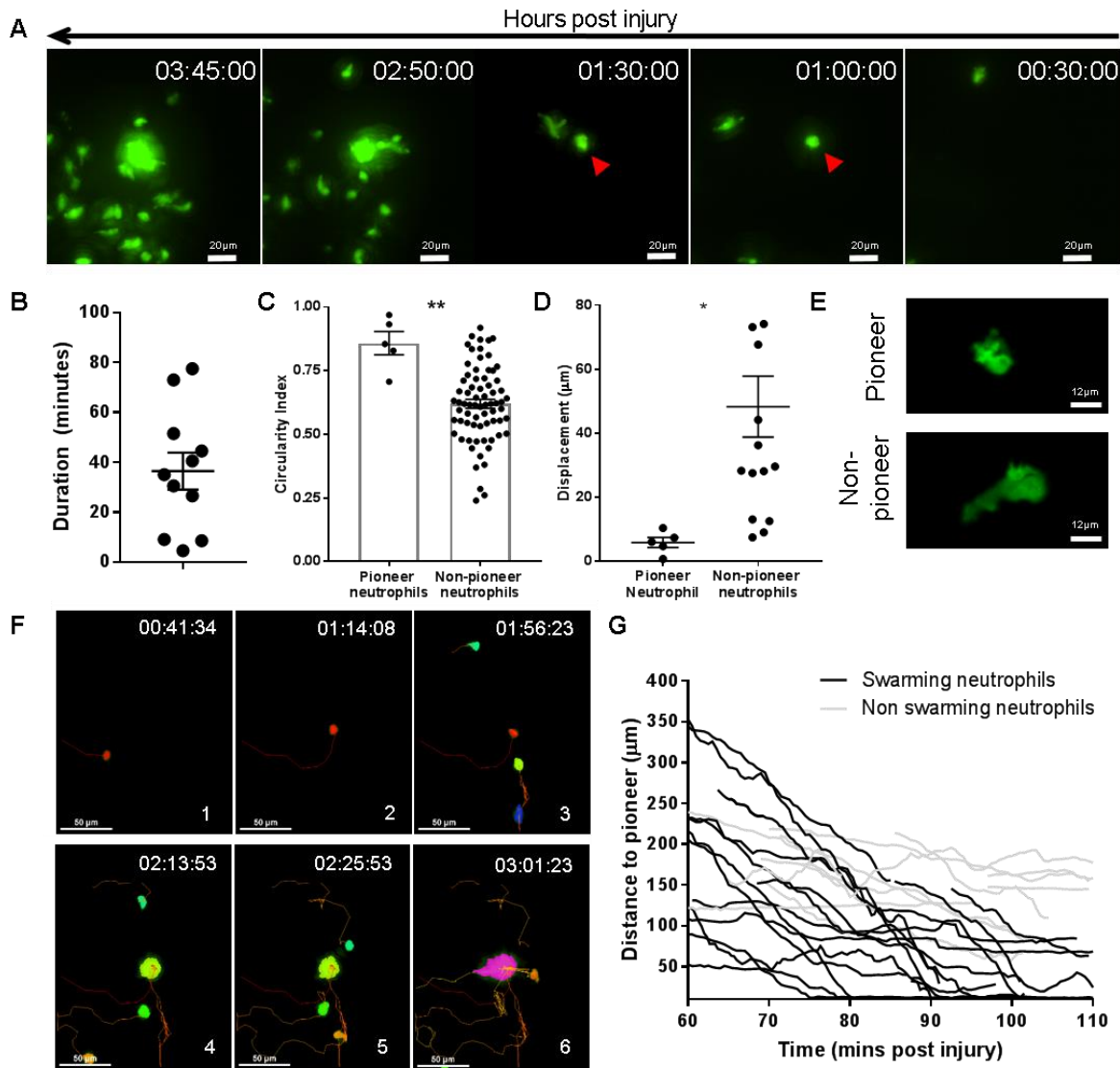
200

201



## 202 **Neutrophil swarms are initiated by a pioneer neutrophil with distinct morphology**

203 The factors which initiate neutrophil swarming are not well defined. Neutrophil swarms in  
204 mammals grow by large-scale migration towards ‘pioneer neutrophils’ in the context of both  
205 sterile inflammation and infection, which likely release additional chemoattractants to initiate  
206 the swarming response<sup>9,11,12</sup>. To understand whether a pioneer neutrophil is distinct to other  
207 early responding neutrophils with a specialised capability to initiate a swarm, the migration  
208 patterns of neutrophils in the time period preceding the swarming response were analysed by  
209 reverse chronological tracking of neutrophil migration to persistent swarms (Figure 3A). The  
210 presence of one individual neutrophil with a distinct morphology was identified in the tissue  
211 region which became the swarm centre in 100% of swarming events examined (Figure 3B-E).  
212 Based on its early recruitment and location at the swarm centre, this neutrophil is referred to  
213 as the pioneer neutrophil. Prior to swarming, the pioneer neutrophil remained stationary in the  
214 tissue region which became the swarm centre for on average  $36 \pm 7$  minutes (Figure 3B).  
215 Pioneer neutrophils were rounded and non-motile, a distinct morphology which is illustrated  
216 by their higher circularity index and lower displacement compared to scouting neutrophils  
217 migrating at the wound site in the frame before swarming (Figure 3C-E). Strikingly in 100% of  
218 swarm initiation events examined, the pioneer neutrophil was the focal point of migration for  
219 swarming neutrophils, whilst non-swarming neutrophils migrated randomly within the wound  
220 region (Figure 3D-E, Supplemental Movie 5).



221

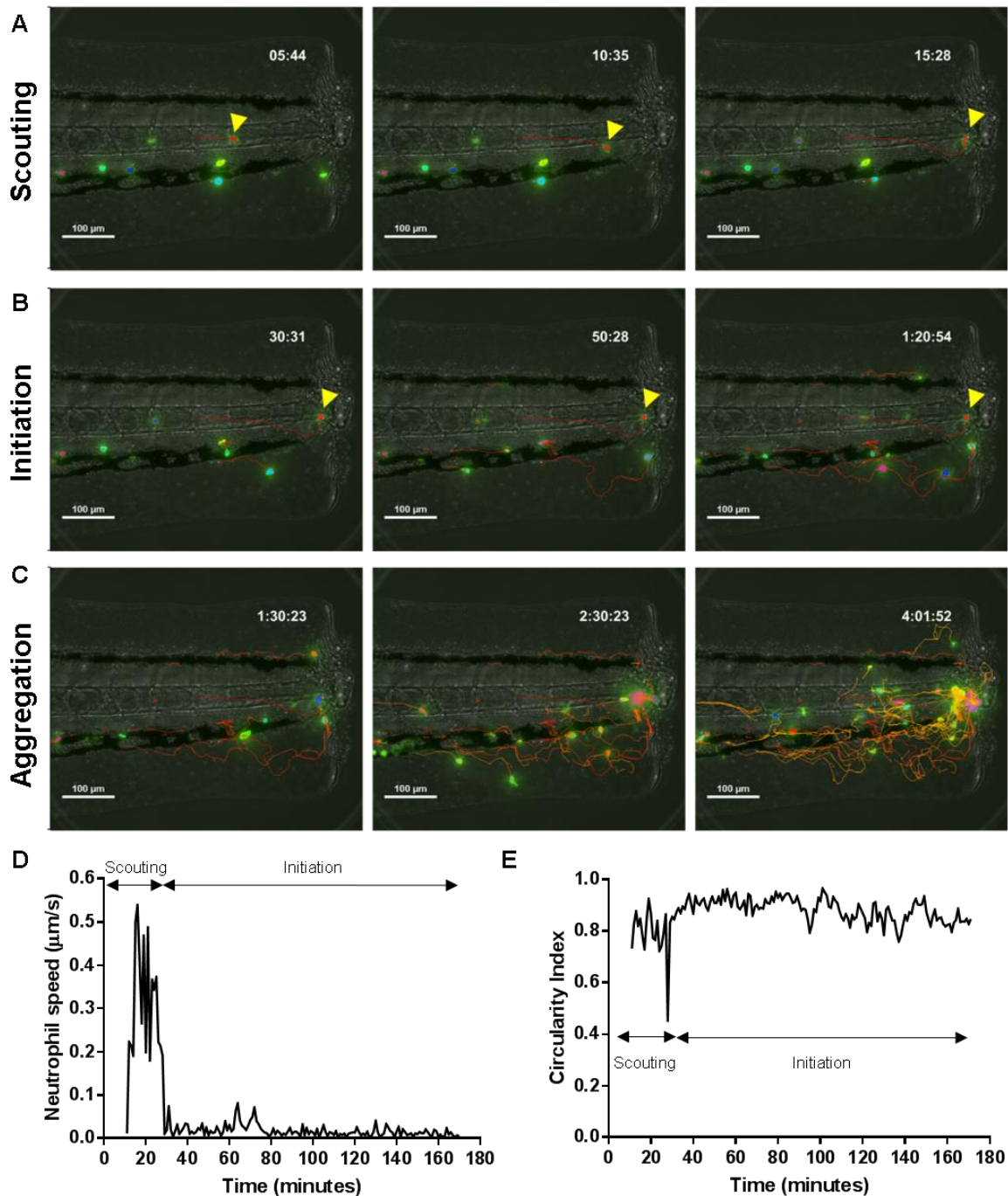
222 **Figure 3. A pioneer neutrophil is the focal point of migration for swarming neutrophils**

223 **A.** Reverse chronological time lapse sequence of a persistent neutrophil swarm where one  
 224 individual neutrophil is visible in the swarm centre prior to neutrophil swarming (red arrows).  
 225 Time stamps shown are hh:mm:ss relative to injury time. **B-E.** Quantification of pioneer  
 226 neutrophil migration pattern in the frames preceding swarming. **B.** Duration pioneer neutrophil  
 227 is observed in the swarm tissue region prior to swarming. **C-D.** The circularity index and  
 228 displacement of pioneer neutrophils and scouting neutrophils migrating at the wound site in  
 229 the same time period ( $n=5$ , unpaired t-test where \*  $p<0.05$  and \*\*  $p<0.01$ ). **E.** Representative  
 230 image (from 5 experiments) of pioneer and non-pioneer neutrophils. **F.** Chronological time  
 231 lapse sequence of swarming neutrophil tracks. The migration of a pioneer neutrophil (red)  
 232 to the wound site is observed (frames 1-2) followed by the directed migration of swarming  
 233 neutrophils towards the pioneer, which is the focal point for migration (frames 3-5). The result

234 of migration is the aggregation of neutrophils to form swarms (frame 6). Tracks are coloured  
235 by time where red corresponds to early and yellow corresponds to late arriving neutrophils. **G.**  
236 Distance-time plot (DTP) of individual cell migration paths of swarming neutrophils (black  
237 tracks) and non-swarming neutrophils at the wound site in the same time period (grey tracks).  
238 Tracks are relative to pioneer neutrophil position; swarming neutrophils migrate to the pioneer  
239 neutrophil whilst non-swarming neutrophils do not (n= 4 independent experiments).

#### 240 **Neutrophil swarming responses to tissue damage occur in three sequential stages**

241 To determine the relationship between the pioneer neutrophil and swarm initiation, neutrophil  
242 migration in the tail-fin at the entire population level was studied. Although there was variation  
243 from fish-to-fish in timing, all swarms formed by: 1) the early recruitment of neutrophils to the  
244 inflammatory site (scouting), 2) the behavioural change of a pioneer neutrophil at the wound  
245 site (initiation), followed by 3) the directed migration of neutrophils to the pioneer to form  
246 swarms (aggregation) (Figure 4, Supplemental Movie 6). Within minutes of injury, neutrophils  
247 began directed migration to the wound site (Figure 4A). This early scouting of neutrophils  
248 lasted on average  $88 \pm 24$  minutes and is consistent with reports in zebrafish<sup>18</sup> and mammalian  
249 systems which describe the recruitment of neutrophils close to the inflammatory site in  
250 response to chemoattractant gradients<sup>9</sup>. Swarm initiation began when the pioneer neutrophil  
251 adopted its rounded, non-motile morphology having arrived at the wound site during the  
252 scouting phase (Figure 4B) and ended when the first neutrophil joined the swarm (on average  
253  $36 \pm 7$  minutes). During the aggregation phase, swarms developed through the directed  
254 migration of neutrophils, which lasted on average  $183 \pm 25$ , or until the end of the imaging  
255 period (Figure 4C). As proof of concept, a non-biased approach was used to study pioneer  
256 neutrophil migration. Pioneer neutrophils were tracked during the time period preceding the  
257 start of swarming, where a change in pioneer neutrophil behaviour was observed, correlating  
258 with the scouting and initiation phases (Figure 4D-E). These stages provide consistent phases  
259 with which to study pioneer neutrophil behaviour between larvae and are comparable to the  
260 swarm stages reported in mammals<sup>9,10</sup>.



261

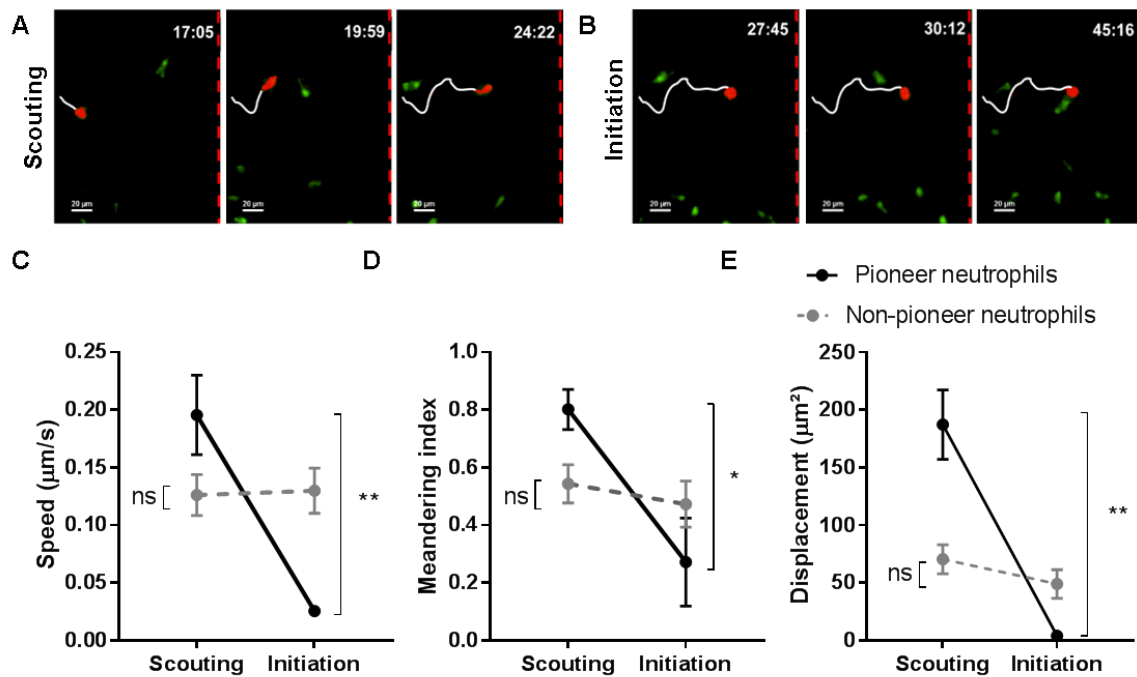
262 **Figure 4. Neutrophil swarming responses to tissue damage occur in three sequential**  
263 **stages**

264 Representative time-lapse sequence (from at least 20 independent observations) showing  
265 coordination of neutrophils to form swarms within the inflamed tail-fin. **A.** Stage 1; scouting.  
266 The recruitment of neutrophils proximal to the wound site occurs within minutes following tail  
267 fin transection. **B.** Stage 2; initiation. Pioneer neutrophils adopt a rounded, non-motile  
268 morphology at the wound site. **C.** Stage 3; aggregation. Neutrophils direct their migration to

269 the pioneer neutrophil which becomes to focal point for migration, resulting in swarm growth  
270 and neutrophil aggregation. Tracks are coloured by time where red corresponds to early and  
271 yellow corresponds to late arriving neutrophils. Time stamps are h:mm:ss relative to the start  
272 of imaging period at 30 minutes post injury. **D-E.** Non-biased approach to observe pioneer  
273 neutrophil behavioural change. **D.** Representative example of pioneer neutrophil migration  
274 speed prior to the swarming response. **E.** Representative example of pioneer neutrophil  
275 circularity index prior to the swarming response. Arrows correspond to the scouting and  
276 initiation phases. Data shown (D-E) corresponds to the pioneer neutrophil illustrated in the  
277 time course sequence (A-C).

### 278 **Pioneer neutrophils adopt a distinct morphology at the wound site**

279 We next investigated whether the morphology observed in pioneer neutrophils prior to  
280 swarming was distinct, or common, to all neutrophils upon arrival at the wound site. Tracks of  
281 neutrophils migrating to the wound site during the scouting and the initiation phases were  
282 extracted (Figure 5A-B) and parameters which describe neutrophil motility including speed,  
283 displacement and meandering index were analysed<sup>15,16</sup>. The speed, displacement and  
284 meandering index of pioneer neutrophils were significantly reduced in the initiation phase  
285 when compared to the scouting phase, whilst neutrophils migrating to the wound site within  
286 the same tissue region did not display this behavioural change (Figure 5C-E). These data  
287 demonstrate that pioneer neutrophils display a distinct morphology at the wound site prior to  
288 swarm formation, which is not seen in scouting neutrophils responding to chemoattractants  
289 produced at the wound edge. Taken together, these findings suggest that within the complexity  
290 of the inflamed tail-fin, specific guidance cues are produced from a single pioneer neutrophil  
291 which enables neutrophils to coordinate their migration to form swarms.



292

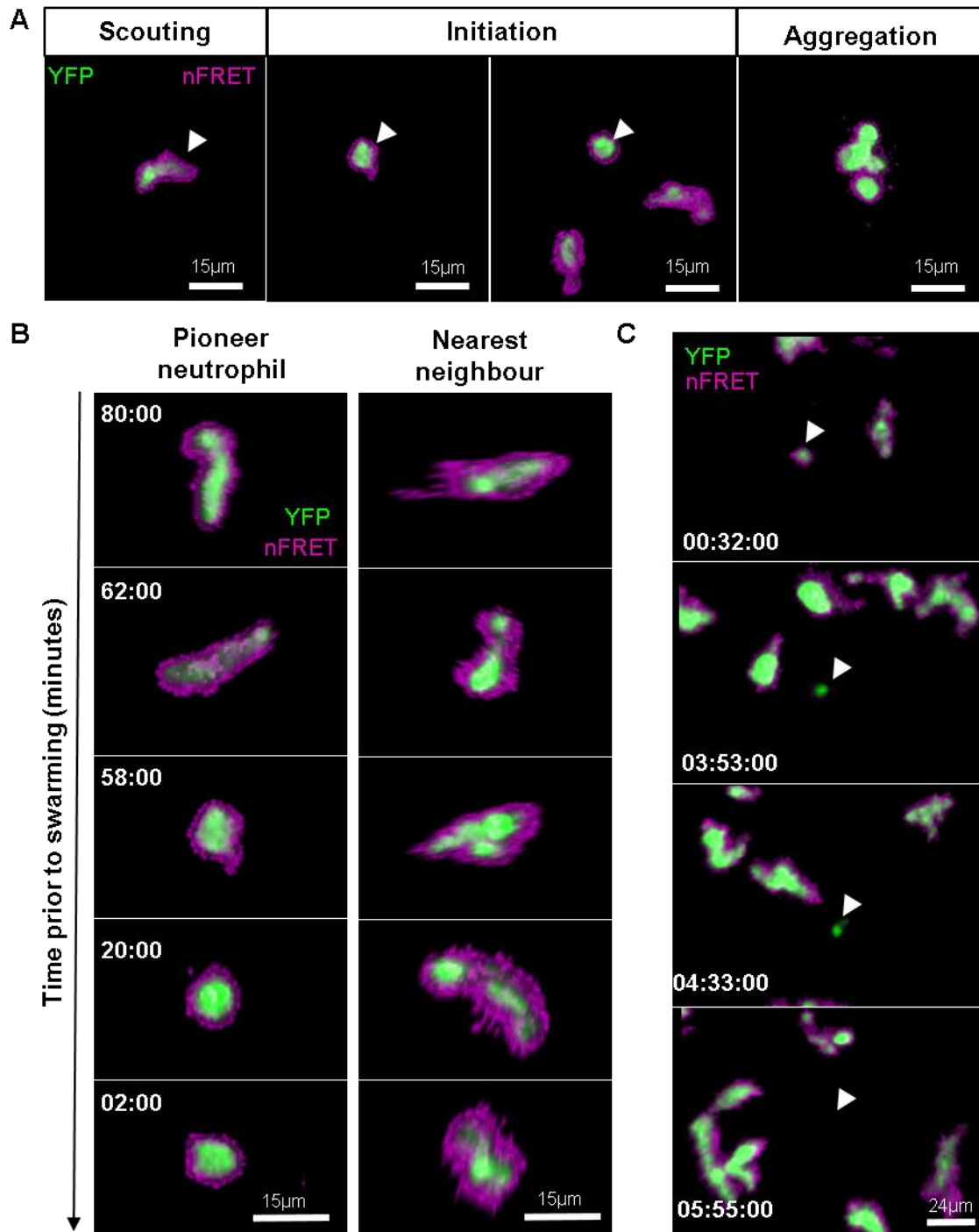
## 293 **Figure 5. Pioneer neutrophils adopt a distinct morphology at the wound site**

294 **A-B.** Representative example of tracking of pioneer neutrophil (highlighted) alongside  
 295 neutrophils migrating within the same time period during the scouting (**A**) and initiation (**B**)  
 296 stages. Wound edge is highlighted by red dashes. **C-E** Parameters to describe neutrophil  
 297 migration were measured. **C.** Neutrophil speed. **D.** Neutrophil displacement (the linear  
 298 distance each neutrophil travelled). **E.** Neutrophil meandering index (the displacement divided  
 299 by the total length of the neutrophil track). Error bars are mean  $\pm$  SEM. Groups were analysed  
 300 using a paired t-test \* $p < 0.05$  \*\* $p < 0.01$ ,  $n = 5$  independent experiments.

## 301 **Pioneer neutrophils are not apoptotic prior to swarming**

302 Cell death signalling has been implicated in neutrophil swarm initiation<sup>9,11</sup>, although the precise  
 303 signals and mode of cell death remain to be determined. The rounded, non-motile morphology  
 304 of pioneer neutrophils is characteristic of an apoptotic neutrophil phenotype previously  
 305 reported<sup>24</sup>. Furthermore apoptotic cells secrete “find-me” and “eat-me” signals to promote the  
 306 attraction of phagocytes for successful removal of apoptotic bodies<sup>25</sup>, therefore we  
 307 hypothesised that cell death signals released by apoptotic neutrophils could initiate the  
 308 swarming response. Neutrophil apoptosis can be studied using the transgenic *Tg(mpx:CFP-*  
 309 *DEVD-YFP)sh237*<sup>24</sup> zebrafish line (known as *mpx:FRET*) which expresses a genetically  
 310 encoded Förster resonance energy transfer (FRET)<sup>26</sup> biosensor consisting of a caspase-3  
 311 cleavable DEVD sequence flanked by a CFP/YFP pair, under the neutrophil-specific *mpx*  
 312 promoter. A loss of FRET signal in this system provides a read out of apoptosis specifically in

313 neutrophils *in vivo* in real time. Analysis of pioneer neutrophils prior to swarming within the tail-  
314 fin (Figure 6A) identified that despite the rounded, non-motile morphology observed in pioneer  
315 neutrophils, a FRET signal was present during both the scouting and initiation phases in all  
316 imaging studies where swarming was observed (Figure 6B, Supplemental Movie 7, n=6  
317 neutrophils from 5 experimental repeats). Furthermore, when an apoptotic event was detected  
318 within the inflamed tail-fin, it was not followed by a neutrophil swarming response (Figure 6C,  
319 Supplemental Movie 8, n=2 neutrophils from 5 experimental repeats). These findings suggest  
320 that neutrophil apoptosis does not initiate neutrophil swarming, and that despite their  
321 morphology, pioneer neutrophils are not undergoing caspase-3 dependent apoptosis. Further  
322 study of neutrophil behaviour in this model using transgenic reporters of cell death will enable  
323 the dissection of the molecular cues which regulate swarm initiation.



324

325 **Figure 6. Pioneer neutrophils are not apoptotic prior to swarming**

326 3dpf *mpx:FRET* larvae were injured and time lapse imaging was performed from 30 minutes  
 327 post injury for 6 hours. Neutrophil signal from the acceptor (green) and nFRET (magenta) are  
 328 shown to illustrate neutrophil apoptosis. **A.** Representative time lapse sequence (from six  
 329 independent observations) illustrating a pioneer neutrophil at the wound site (white arrow)  
 330 during the scouting and initiation phases prior to swarming in *mpx:FRET* larvae. **B.** Pioneer



331 neutrophils are not apoptotic. Representative example (from six independent observations) of  
332 a pioneer neutrophil and its nearest neighbour in the frames preceding neutrophil swarming.  
333 The initiation stage is observed 58 minutes prior to swarming (rounded pioneer neutrophil).  
334 nFRET signal is intact at all stages of migration prior to swarming in both the pioneer and  
335 nearest-neighbour non-pioneer neutrophil. Time stamps are mm:ss relative to the swarm start  
336 time. **C.** Apoptotic neutrophils do not initiate swarming. Representative example of neutrophil  
337 apoptosis (from 2 independent observations) at the wound site demonstrated by loss of FRET  
338 signal around 4 hours post injury, followed by the absence of neutrophil cluster formation in  
339 the same tissue region by the end of the imaging period. Time stamp is relative to injury time  
340 and is hh:mm:ss.

## 341 **Discussion**

342 In this study we investigated the migration patterns of neutrophils in the context of  
343 inflammation and infection and identified that neutrophil swarming behaviour is conserved in  
344 zebrafish immunity. We focused on neutrophil swarming in the context of injury-induced  
345 inflammation, where the zebrafish model allowed us to track endogenous neutrophils in a  
346 physiologically relevant tissue damage model *in vivo*. Here, we identified three stages of  
347 migration leading to swarming, where the altered behaviour of one individual neutrophil was  
348 sufficient to induce a swarming response in a significant proportion of larvae.

349 We utilised the optical transparency of zebrafish larvae to precisely track neutrophils over time,  
350 providing some of the first *in vivo* characterisation of endogenous neutrophil migration patterns  
351 in response to tissue injury since the identification of neutrophil swarming. Currently our  
352 knowledge of swarm initiation is based on mouse models using transfer of exogenous  
353 neutrophils into the ear dermis followed by focal laser injury. These studies adopt the transfer  
354 of neutrophils from a variety of donor backgrounds, enabling the screening of many candidate  
355 signalling pathways, and have thus been invaluable for understanding the molecular control  
356 of swarming at the later stages<sup>11,12</sup>. However, transplanted neutrophils bypass the early  
357 recruitment, priming and activation stages with which endogenous neutrophils undergo as  
358 they egress from the bloodstream, making the early stages of swarming difficult to dissect.  
359 The zebrafish model circumvents these limitations, enabling the visualisation of endogenous  
360 neutrophil migration from their physiological tissue niche.

361 Neutrophil responses to tissue injury are thought to occur in phases: the early recruitment of  
362 neutrophils (referred to as 'scouting') is followed by the large scale synchronised migration of  
363 neutrophils from distant regions (amplification), resulting in large scale tissue infiltration from  
364 the bloodstream<sup>9-11</sup>. We demonstrate in our model that neutrophil response to tail fin  
365 inflammation is bi-phasic; neutrophils proximal to the wound edge are recruited within minutes

366 following injury, whilst neutrophils from further away recruited between 2-6 hours following  
367 injury. This is reminiscent of the bi-phasic neutrophil response to focal tissue damage  
368 described in mice<sup>9,11</sup>. The time period of 6 hours required for recruitment in our system likely  
369 reflects the difference in assays adopted between our study and mammalian studies; the  
370 propagation of signals through the whole animal is required for neutrophil migration from tissue  
371 niches in zebrafish whilst in mammals, neutrophils are injected proximal to the damage site.  
372 In mammals, early neutrophil recruitment is modulated by signals released from damaged or  
373 necrotic cells which are likely to be damage-associated molecular patterns (DAMPs). These  
374 DAMPs include DNA, histones, interleukin-1 $\alpha$  (IL-1 $\alpha$ ), N-formyl peptides and Adenosine  
375 triphosphate (ATP) (reviewed in <sup>27</sup>). These signals can be short-lived<sup>17</sup>, so the production of  
376 longer term signals is required for sustained neutrophil recruitment<sup>28</sup>. LTB4 is a signal-relay  
377 molecule which acts over long distances to promote neutrophil recruitment to formyl peptides  
378 released from the centre of inflammatory sites<sup>14</sup>. We inhibited LTB4 signalling by targeting the  
379 LTA4H enzyme or the LTB4 receptor using CRISPR/Cas9 and found neutrophil responses  
380 were impaired only in the later stages of recruitment (3-6hpi). In zebrafish the CRISPR/Cas9  
381 system is highly efficient, resulting in biallelic gene disruption in F0 zebrafish embryos which  
382 allows for direct phenotypic analysis of injected animals<sup>22</sup>. Based on the expression of *Ita4h*  
383 and *blt1* on neutrophils we propose that disruption of these genes will affect neutrophil  
384 production and detection of LTB4. Our data agree with those from mice studies, showing that  
385 the recruitment of neutrophils deficient in the LTB4 receptor is impaired only in neutrophils  
386 distant to the focal tissue injury, whilst those proximal to the wound site are recruited like  
387 wildtype neutrophils<sup>11</sup>. Evidence from zebrafish studies have demonstrated that following tail-  
388 fin transection, gradients of neutrophil chemoattractant signals are produced within minutes,  
389 which extend up to 200 $\mu$ m into the tail fin epithelium as a concentration gradient<sup>17</sup>. Hydrogen  
390 peroxide and chemokines such as CXCL8 are known to be important in neutrophil recruitment  
391 in zebrafish larvae<sup>17,29</sup>. We therefore propose that the initial recruitment of neutrophils to the  
392 wound site is dependent on the release of these chemoattractants, whilst signalling through  
393 LTB4 is required to attract neutrophils at later stages from more distant tissue regions.

394 Factors which are likely to influence the swarm outcome include the size of the initiating tissue  
395 damage, the presence of pathogens in the tissue, induction of secondary cell death and the  
396 number of neutrophils initially recruited<sup>19</sup>. Linear tail-fin transection avoids creating a focal  
397 source of neutrophil chemoattractants, migration towards which could mimic a swarming  
398 response without the requirement for neutrophil-neutrophil signalling. Based on our findings  
399 we propose that the formation of neutrophil swarms within a complex environment of diffusing  
400 chemotactic gradients at the wound site would be dependent on intercellular signalling  
401 between neutrophils. The zebrafish model therefore is a truly physiological system in which to

402 study the early events that determine the outcome of neutrophil swarming. Within the inflamed  
403 tail-fin tissue, we found that neutrophil swarms developed around one individual neutrophil.  
404 The single-cell resolution achieved in our study enabled us to make the striking observation  
405 that this pioneer neutrophil adopted a distinct morphology at the wound site prior to swarming.  
406 Other groups have found that within inflamed or infected interstitial tissue, the initial arrest of  
407 a small number of 'pioneer' or 'scouting' neutrophils precedes a later influx of neutrophil  
408 migration<sup>11,12</sup>. In these studies, it is unclear whether pioneer neutrophils are simply early  
409 responding 'scouting' neutrophils, or if they have a specialised capacity for swarm initiation.  
410 Based on our observations, we distinguished pioneer neutrophils from other scouting  
411 neutrophils and propose that pioneer neutrophils have specialised functions required for  
412 swarm initiation, whilst scouting neutrophils are simply early responders to chemoattractants  
413 produced by damaged cells or pathogens at the inflammatory site.

414 Neutrophil swarming at the wound site in our system occurred in three distinct stages, which  
415 are comparable to the sequential phases described in the swarming of neutrophils in  
416 intravenous/ intradermal transfer models in mice<sup>9,30</sup>. Ng et al. describe a three phase cascade  
417 of events to describe neutrophil migration towards laser induced or sterile needle induced  
418 tissue injury<sup>9</sup>, which was further adapted into a five step attraction model<sup>30</sup>. In our linear tail-  
419 fin model we found that migration patterns leading to swarming shares features of both  
420 models. During the scouting phase we observed the chemotactic movement of neutrophils  
421 proximal to the wound site, sharing features with the scouting observed in mice and human  
422 neutrophils<sup>9,10</sup>. The initial recruitment of neutrophils proximal to the wound site is common to  
423 inflammation induced by infection or tissue injury, where these neutrophil 'scouts' are likely  
424 responding to gradients of chemoattractants produced by damaged cells or pathogens<sup>9,10</sup>.  
425 One pioneer neutrophil within the inflamed tail-fin was sufficient to initiate swarming in  
426 zebrafish larvae, sharing function with the pioneer neutrophils essential for swarm initiation in  
427 mice<sup>30</sup>. Due to the relatively few number of neutrophils present in zebrafish larvae (~300) in  
428 comparison with the thousands ( $2-5 \times 10^4$ )<sup>9</sup> injected into the mouse ear, we propose that  
429 signals generated from just one pioneer neutrophil are sufficient to drive a swarming response  
430 in our system. The pioneer behavioural change was observed during the swarm 'initiation'  
431 phase. The initiation phase encapsulates the time period in which the pioneer neutrophil  
432 adopted a rounded non-motile morphology at the wound site, until the first swarming neutrophil  
433 makes contact. We propose that this stage is comparable to stage 2 'swarm amplification by  
434 cell death' reported in mice<sup>30</sup>. Following its arrest, we observed directed migration of  
435 neutrophils towards the pioneer during the aggregation phase which lasted until the end of the  
436 imaging period in many larvae. The aggregation phase corresponds to the aggregation phase  
437 reported by Lammermann<sup>30</sup>, and the cluster 'stabilisation' phase described by Ng<sup>9</sup>. The

438 parallels between the migration patterns leading swarming in zebrafish with those reported in  
439 mice<sup>9,30</sup> and humans<sup>10</sup> suggests that the initiation of swarming is conserved between species.  
440 Furthermore, these stages provide measurable time periods for the comparison of neutrophil  
441 behaviour in future experiments to determine the signals released by pioneer neutrophils.

442 Based on the morphology of pioneer neutrophils we investigated whether neutrophil apoptosis  
443 generated the chemoattractant signals required to initiate a swarming response within the tail-  
444 fin. Interestingly caspase-3 was intact during the swarm initiation phase, indicating that swarm  
445 initiating pioneer neutrophils were not undergoing neutrophil apoptosis prior to swarming. Due  
446 to the requirement for live imaging to study pioneer neutrophils prior to swarming, it was not  
447 technically possible to confirm our results using staining assays such as TUNEL. However,  
448 other studies have found that results using the *mpx:FRET* transgenic line recapitulate TUNEL  
449 staining<sup>24</sup>, suggesting this is a reliable way to read out neutrophil apoptosis. The successful  
450 application of the FRET transgenic reporter line to study apoptosis during swarm initiation  
451 identifies that it is possible to study neutrophil swarm initiation in different reporter lines, which  
452 will be useful in future to investigate other cell death signals important for swarm initiation. It  
453 has been proposed that within the interstitium, neutrophils must prioritise 'superior'  
454 chemoattractant gradients in order to home towards sites of necrosis or infection, sparing the  
455 surrounding viable tissue<sup>27</sup>. The presence of pathogens in the tissue or induction of secondary  
456 cell death are factors which influence neutrophil swarming<sup>19</sup>. Neutrophils integrate and  
457 prioritise chemoattractive cues where there appears to exist a hierarchical preference for  
458 bacterial derived end-point chemoattractants, such as formyl peptides, over endogenous  
459 intermediary gradients such as CXCL8 and LTB4<sup>31,32</sup>. The behavioural change observed in  
460 the swarm initiating pioneer, but not scouting neutrophils, suggests that pioneer neutrophils  
461 encounter a tissue environment which induces their behavioural change. Our findings suggest  
462 that pioneer neutrophils arrive at the wound site where they release chemoattractant  
463 molecules which are prioritised by a population of neutrophils, resulting in coordinated  
464 migration within the inflamed tissue region to form swarms (summarised in supplemental figure  
465 7). The pioneer signals could be derived through the activation of a cell death pathway, the  
466 presence of a pathogen in the inflamed tissue, or a combination of both. Lysis of neutrophils  
467 corresponds with rapid migration of neutrophils within seconds in mice, suggesting a role for  
468 'necrotaxis' in mediating neutrophil migration<sup>12</sup>. Furthermore, cell death and subsequent DNA  
469 release is observed at sites of alum injection associated with neutrophil swarming in mice,  
470 suggesting that cell death by NETosis may be important in swarming<sup>33</sup>. Pioneer neutrophils in  
471 our study appeared to be viable prior to swarming, suggesting that lysis is not an initiating  
472 factor in this model, although a programmed cell death process such as apoptosis or NETosis

473 is possible. Given that neutrophils respond to a multitude of chemoattractant signals, it is likely  
474 that the release of multiple signals could be responsible for swarming behaviour.

475 Our findings in this study suggest that the zebrafish model of neutrophil swarming will be  
476 extremely useful in dissecting the signalling which modulates early stages of neutrophil  
477 swarming. Measuring and inhibiting intercellular signalling molecules is technically challenging  
478 *in vivo*, posing significant barriers to dissecting the modulators of swarming at different stages.  
479 Further elucidation of the nature of the pioneer neutrophil will require the development of new  
480 technologies for the read-out of cell death phenomena and cytokine production *in vivo*. Using  
481 a combination of transgenic zebrafish lines expressing cell-death read outs in neutrophils and  
482 cell viability dyes, we will investigate pioneer neutrophil death as a potential mechanism for  
483 swarm-initiation. Furthermore, the development of CRISPR interference technology and  
484 neutrophil specific drivers of dead Cas9 by our group will enable us to inhibit genes of interest  
485 in neutrophils specifically for loss-of-function studies, to identify the signals important in early  
486 swarm initiation. These techniques will bypass limitations of other systems to allow the  
487 dissection of early-swarming signals *in vivo*.

488 Understanding why swarms are initiated will be important for understanding the signals which  
489 control the coordination of neutrophil migration within interstitial tissues. Our findings identify  
490 that neutrophil swarm initiation at sites of tissue damage requires signals from one pioneer  
491 neutrophil and that these signals can be dissected in future using the zebrafish model.

492

## 493 **Materials and methods**

### 494 Zebrafish husbandry and ethics

495 To study neutrophils during inflammation *Tg(mpx:EGFP)i114* (known as *mpx:GFP*) zebrafish  
496 larvae were in-crossed. All zebrafish were raised in the Bateson Centre at the University of  
497 Sheffield in UK Home Office approved aquaria and maintained following standard protocols<sup>34</sup>.  
498 Tanks were maintained at 28°C with a continuous re-circulating water supply and a daily  
499 light/dark cycle of 14/10 hours. All procedures were performed on embryos less than 5.2 dpf  
500 which were therefore outside of the Animals (Scientific Procedures) Act, to standards set by  
501 the UK Home Office.

### 502 Tail-fin transection assay

503 To induce an inflammatory response, zebrafish larvae at 2 or 3dpf were anaesthetised in  
504 Tricaine (0.168 mg/ml; Sigma-Aldrich) in E3 media and visualised under a dissecting  
505 microscope. Tail-fins were transected consistently using a scalpel blade (5mm depth, WPI) by  
506 slicing immediately posterior to the circulatory loop, ensuring the circulatory loop remained  
507 intact as previously described<sup>18</sup>.

### 508 Widefield microscopy of transgenic larvae

509 For neutrophil tracking experiments, injured 3dpf *mpx:GFP* larvae were mounted in a 1% low  
510 melting point agarose solution (Sigma-Aldrich) containing 0.168 mg/ml tricaine immediately  
511 following tail fin transection. Agarose was covered with 500µl of a clear E3 solution containing  
512 0.168 mg/ml tricaine to prevent dehydration. Time lapse imaging was performed from 0.5-5  
513 hours post injury with acquisition every 30 seconds using 10 z-planes were captured per larvae  
514 over a focal range of 100µm using an Andor Zyla 5 camera (Nikon) and a GFP specific filter  
515 with excitation at 488nm. Maximum intensity projections were generated by NIS elements  
516 (Nikon) to visualise all 10 z-planes.

### 517 Confocal microscopy of transgenic larvae

518 For visualising neutrophil swarming at high magnification, larvae were mounted in a 1% low  
519 melting point agarose solution (Sigma-Aldrich) containing 0.168 mg/ml tricaine for imaging  
520 immediately after tail transection. Agarose was covered with 2000µl of clear E3 solution  
521 containing 0.168 mg/ml tricaine to prevent dehydration. Imaging was performed from 30  
522 minutes post injury using a 20x or 40x objective on an UltraVIEWVoX spinning disc confocal  
523 laser imaging system (Perkin Elmer). Fluorescence for GFP was acquired using an excitation

524 wavelength of 488nm and emission was detected at 510nm, and fluorescence for mCherry  
525 was acquired using 525nm emission and detected at 640nm. Images were processed using  
526 Volocity™ software.

#### 527 Tracking assays

528 Tracking of GFP labelled neutrophils was performed using NIS Elements (Version 4.3) with  
529 an additional NIS elements tracking module. A binary layer was added to maximum intensity  
530 projections to detect objects. Objects were smoothed, cleaned and separated to improve  
531 accuracy. A size restriction was applied where necessary to exclude small and large objects  
532 which did not correspond to individual neutrophils.

#### 533 Distance-time plots

534 For wound plots the distances from the wound were obtained by processing neutrophil tracks  
535 under the assumption that the tail fin wound is a straight line parallel to the x-axis of the  
536 greyscale image. Neutrophil tracking data was extracted from NIS elements and imported into  
537 MatLab software. For distance to pioneer plots the pioneer centre was set as a reference point  
538 and tracking was performed to determine neutrophil distance to the reference point. Tracks  
539 were extracted from NIS elements and plotted manually using GraphPad Prism version 7.0.

#### 540 Neutrophil specific expression of zebrafish genes

541 Gene expression was assessed using an RNA sequencing database from FACS sorted GFP  
542 positive cells from 5dpf zebrafish<sup>35</sup> (data deposited on GEO under accession number  
543 GSE78954). RPKM values for genes of interest were extracted. For single cell analysis gene  
544 expression values were extracted from the BASiCz (Blood atlas of single cells in zebrafish)  
545 cloud repository<sup>36</sup>. Cells of the neutrophil lineage were analysed for gene expression based of  
546 LTB4 signalling components.

#### 547 CRISPR/Cas9 reagents

548 Synthetic SygRNA® (crRNA and tracrRNA) (Merck) in combination with cas9 nuclease protein  
549 (Merck) was used for gene editing. Transactivating RNAs (tracrRNA) and gene specific  
550 CRISPR RNAs (crRNA) were resuspended to a concentration of 20µM in nuclease free water  
551 containing 10mM Tris-hcl pH8. SygRNA® complexes were assembled on ice immediately  
552 before use using a 1:1:1 ratio of crRNA:tracrRNA:Cas9 protein. Gene-specific crRNAs to  
553 target the ATG region of *blt1* and *Ita4h* were designed using the online tool CHOPCHOP  
554 (<http://chopchop.cbu.uib.no/>). We used the following crRNA sequences targeting the ATG

555 region of both genes, where the PAM site is indicated in brackets: *Ita4h*:  
556 AGGGTCTGAAACTGGAGTCA(TGG), *blt1*: CAATGCCAATCTGATGGGAC(AGG).

557 Microinjection of SygRNA® into embryos

558 A 1nl drop of SygRNA®:Cas9 protein complex was injected into *mpx*:GFP embryos at the one-  
559 cell stage. Embryos were collected at the one cell stage and injected using non-filament glass  
560 capillary needles (Kwik-Fil™ Borosilicate Glass Capillaries, World Precision Instruments  
561 (WPI), Herts, UK). RNA was prepared in sterile Eppendorf tubes. A graticule was used to  
562 measure 0.5nl droplet sizes to allow for consistency of injections. Injections were performed  
563 under a dissecting microscope attached to a microinjection rig (WPI) and a final volume of 1nl  
564 was injected.

565 Genotyping and melting curve analysis

566 Site-specific mutations were detected using High Resolution Melting (HRM) Analysis which  
567 can reliably detect CRISPR/Cas9 induced indels in embryos<sup>37,38</sup>. Genomic DNA extraction  
568 was performed on larvae at 2dpf. Larvae were placed individually in 0.2ml PCR tubes in 90µl  
569 50mM NaOH and boiled at 95° for 20 minutes. 10µl Tris-HCL pH8 was added as a reaction  
570 buffer and mixed thoroughly. Gene specific primers were designed using the Primer 3 web  
571 tool (<http://primer3.ut.ee/>). Sequences were as follows *Ita4h\_fw*:  
572 CGTGTAGGTTAAAATCCATTCGCA *Ita4h\_rev*: GAGAGCGAGGAGAAGGAGCT *blt1\_fw*:  
573 GTCTTCTCTGGACCACCTGC *blt1\_rev*: ACACAAAAGCGATAACCAGGA. HRM analysis  
574 (Bio-Rad) PCR reactions were made with 5µl Sybr™ Green master mix (Thermo Fisher), 0.5µl  
575 of each primer (10µM), 1µl gDNA and 3µl water to make a final reaction volume of 10µl. PCR  
576 reactions were performed in a LightCycler instrument (Bio-Rad) using 96-well plates. The two-  
577 step reaction protocol was as follows: 95 °C for 2 min, followed by 35 cycles of 95 °C for 10  
578 seconds, 58° for 30 seconds, 72° for 20 seconds. The second stage of the protocol was 95 °C  
579 for 30 seconds, 60 °C for 60 seconds, 65 °C for 10 seconds. The temperature then increased  
580 by 0.02 °C/s until 95 °C for 10 seconds. Melt curves were analysed using Bio-Rad software  
581 version 1.2. Successful detection of CRISPR/Cas9 induced indels is illustrated in supplemental  
582 figure 6. Mutagenesis frequencies of 91% and 88% were detected for *Ita4h* and *blt1*  
583 respectively.

584 *Staphylococcus aureus* preparation

585 *Staphylococcus aureus* strain SH1000 pMV158mCherry was used for all experiments<sup>39</sup>. An  
586 overnight bacterial culture was prepared by growing 1cfu of SH1000 pMV158mCherry in



587 10mLs of bovine heart medium (BHI) (Sigma Aldrich lot number 53286) and 10 $\mu$ Ls of 5mg/mL  
588 tetracycline (Sigma-Aldrich) for 16-18 hours at 37°C. 500 $\mu$ Ls of this overnight culture was then  
589 aliquoted into 50mLs of BHI (Sigma Aldrich, 53286) infused with 50 $\mu$ Ls of 5mg/mL tetracycline  
590 (Sigma Aldrich) and grown until an optical density at 600nm of 0.5 was obtained. This culture  
591 was pelleted and resuspended in PBS (pH 7.4) (Fisher Scientific lot number 1282 1680) to a  
592 concentration of 2500cfu per nL.

593 Otic vesicle injection

594 2500cfu of Sh1000 pMV158mCherry was injected into the left otic vesicle of 2dpf  
595 *Tg(mpx:GFP)i114* larvae. A graticule was used to measure 0.5nl droplet sizes to allow for  
596 consistency of injections. Injections were performed under a dissecting microscope attached  
597 to a microinjection rig (WPI) and a final volume of 1nl was injected. For analysis of swarm  
598 volumes larvae were fixed in 4% paraformaldehyde in PBS and imaged using a spinning disk  
599 confocal microscope.

600 Förster resonance energy transfer imaging of neutrophil apoptosis

601 To visualise apoptotic events in the context of neutrophil swarming, 3dpf *Tg(mpx:CFP-DEVD-*  
602 *YFP)sh237* (known as *mpx:FRET*) were injured and mounted in a 1% agarose solution  
603 containing 0.168 mg/ml tricaine and covered with 500 $\mu$ l of a clear E3 solution containing  
604 tricaine to prevent dehydration.

605 FRET imaging was performed from 30 minutes post injury for 5 hours using a 20x objective  
606 lens on an UltraVIEWVoX spinning disc confocal laser imaging system (Perkin Elmer) with  
607 acquisition every 2 minutes. 10 z-planes were captured per larvae over a focal range of 100 $\mu$ m  
608 using the following filters: a donor CFP channel (440nm for excitation, 485nm for detection),  
609 an acceptor YFP channel (514nm for excitation and 587nm for detection), and a FRET channel  
610 (440nm for excitation and 587nm for detection). An Ultraview dichroic mirror passes  
611 405,440,515,640 was used to increase imaging speed using these filter blocks. Velocity™  
612 software was used to calculate normalised FRET values (nFRET). To compensate for the  
613 bleed through of the CFP and YFP fluorophores into the FRET channel, FRET bleed through  
614 constants were calculated. Control samples containing HeLa cells transfected with CFP alone  
615 or YFP alone were imaged using the same settings used for data acquisition of the *mpx:FRET*  
616 zebrafish reporter line. ROIs were drawn around a population of cells in the frame and  
617 Velocity™ software calculated FRET bleed through values as the mean intensity of the  
618 recipient channel (FRET) divided by the mean intensity of the source (CFP or YFP). These

619 FRET constants were then used by Volocity™ to calculate a normalised FRET value.  
620 Neutrophil apoptosis was observed by overlaying the YFP and nFRET channels.

621 Statistical analysis

622 Data were analysed using GraphPad Prism version 7.0. Paired *t* tests were used for  
623 comparisons between two groups and one-way ANOVA with appropriate post-test adjustment  
624 was used for comparisons of three or more groups.

## 625 **Acknowledgements**

626 The authors would like to thank The Bateson Centre Aquarium Team at the University of  
627 Sheffield for fish upkeep. Thank you to the Wolfson Light Microscopy Facility and Darren  
628 Robertson for imaging advice and upkeep of microscopy facilities. We are grateful to Tomasz  
629 Prajsnar for providing *S. aureus* strains.

## 630 **Competing Interests**

631 The authors declare no conflict of interest.

## 632 **References**

- 633 1. Rock KL, Latz E, Ontiveros F, Kono H. The sterile inflammatory response. *Annu Rev*  
634 *Immunol.* 2010;28:321-342. doi:10.1146/annurev-immunol-030409-101311
- 635 2. Urban CF, Reichard U, Brinkmann V, Zychlinsky A. Neutrophil extracellular traps  
636 capture and kill *Candida albicans* and hyphal forms. *Cell Microbiol.* 2006;8(4):668-  
637 676. doi:10.1111/j.1462-5822.2005.00659.x
- 638 3. Wang J. Neutrophils in tissue injury and repair. *Cell Tissue Res.* 2018;371(3):531-  
639 539. doi:10.1007/s00441-017-2785-7
- 640 4. Ley K, Laudanna C, Cybulsky MI, Nourshargh S. Getting to the site of inflammation:  
641 the leukocyte adhesion cascade updated. *Nat Rev Immunol.* 2007;7(9):678-689.  
642 doi:10.1038/nri2156
- 643 5. Woodfin A, Voisin M-B, Nourshargh S. Recent developments and complexities in  
644 neutrophil transmigration. *Curr Opin Hematol.* 2010;17(1):9-17.  
645 doi:10.1097/MOH.0b013e3283333930
- 646 6. Nourshargh S, Alon R. Leukocyte Migration into Inflamed Tissues. *Immunity.*  
647 2014;41(5):694-707. doi:10.1016/J.IMMUNI.2014.10.008

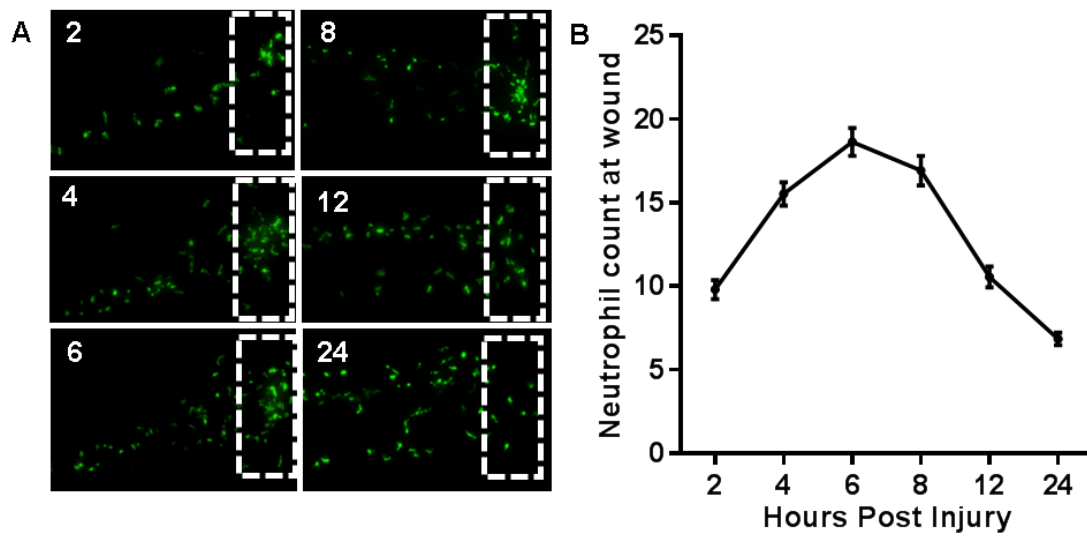
- 648 7. Condliffe AM, Kitchen E, Chilvers ER. Neutrophil priming: pathophysiological  
649 consequences and underlying mechanisms. *Clin Sci (Lond)*. 1998;94(5):461-471.  
650 <http://www.ncbi.nlm.nih.gov/pubmed/9682667>. Accessed December 3, 2018.
- 651 8. McDonald B, Kubes P. Chemokines: Sirens of Neutrophil Recruitment—but Is It Just  
652 One Song? *Immunity*. 2010;33(2):148-149. doi:10.1016/J.IMMUNI.2010.08.006
- 653 9. Ng LG, Qin JS, Roediger B, et al. Visualizing the neutrophil response to sterile tissue  
654 injury in mouse dermis reveals a three-phase cascade of events. *J Invest Dermatol*.  
655 2011;131(10):2058-2068. doi:10.1038/jid.2011.179
- 656 10. Reátegui E, Jalali F, Khankhel AH, et al. Microscale arrays for the profiling of start and  
657 stop signals coordinating human-neutrophil swarming. *Nat Biomed Eng*.  
658 2017;1(7):0094. doi:10.1038/s41551-017-0094
- 659 11. Lämmermann T, Afonso P V, Angermann BR, et al. Neutrophil swarms require LTB<sub>4</sub>  
660 and integrins at sites of cell death in vivo. 2013. doi:10.1038/nature12175
- 661 12. Chtanova T, Schaeffer M, Han S-J, et al. Dynamics of Neutrophil Migration in Lymph  
662 Nodes during Infection. *Immunity*. 2008;29(3):487-496.  
663 doi:10.1016/j.immuni.2008.07.012
- 664 13. Peters NC, Egen JG, Secundino N, et al. In vivo imaging reveals an essential role for  
665 neutrophils in leishmaniasis transmitted by sand flies. *Science*. 2008;321(5891):970-  
666 974. doi:10.1126/science.1159194
- 667 14. Afonso P V., Janka-Junttila M, Lee YJ, et al. LTB<sub>4</sub> Is a Signal-Relay Molecule during  
668 Neutrophil Chemotaxis. *Dev Cell*. 2012;22(5):1079-1091.  
669 doi:10.1016/j.devcel.2012.02.003
- 670 15. Robertson AL, Holmes GR, Bojarczuk AN, et al. A zebrafish compound screen  
671 reveals modulation of neutrophil reverse migration as an anti-inflammatory  
672 mechanism. *Sci Transl Med*. 2014;6(225):225ra29. doi:10.1126/scitranslmed.3007672
- 673 16. Loynes CA, Lee JA, Robertson AL, et al. PGE<sub>2</sub> production at sites of tissue injury  
674 promotes an anti-inflammatory neutrophil phenotype and determines the outcome of  
675 inflammation resolution in vivo. *Sci Adv*. 2018;4(9):eaar8320.  
676 doi:10.1126/sciadv.aar8320
- 677 17. Niethammer P, Grabher C, Look AT, Mitchison TJ. A tissue-scale gradient of  
678 hydrogen peroxide mediates rapid wound detection in zebrafish. *Nature*.  
679 2009;459(7249):996-999. doi:10.1038/nature08119

- 680 18. Renshaw S, Loynes C. A transgenic zebrafish model of neutrophilic inflammation.  
681 *Blood*.... 2006;108(13):3976-3978. doi:10.1182/blood-2006-05-024075.
- 682 19. Kienle K, Lämmermann T. Neutrophil swarming: an essential process of the  
683 neutrophil tissue response. *Immunol Rev*. 2016;273(1):76-93. doi:10.1111/imr.12458
- 684 20. Tobin DM, Vary JC, Ray JP, et al. The *Ita4h* locus modulates susceptibility to  
685 mycobacterial infection in zebrafish and humans. *Cell*. 2010;140(5):717-730.  
686 doi:10.1016/j.cell.2010.02.013
- 687 21. Chatzopoulou A, Heijmans JPM, Burgerhout E, et al. Glucocorticoid-Induced  
688 Attenuation of the Inflammatory Response in Zebrafish. *Endocrinology*.  
689 2016;157(7):2772-2784. doi:10.1210/en.2015-2050
- 690 22. Jao L-E, Wente SR, Chen W. Efficient multiplex biallelic zebrafish genome editing  
691 using a CRISPR nuclease system. *Proc Natl Acad Sci*. 2013;110(34):13904-13909.  
692 doi:10.1073/pnas.1308335110
- 693 23. Kamenyeva O, Boullaran C, Kabat J, et al. Neutrophil Recruitment to Lymph Nodes  
694 Limits Local Humoral Response to *Staphylococcus aureus*. McLoughlin RM, ed.  
695 *PLOS Pathog*. 2015;11(4):e1004827. doi:10.1371/journal.ppat.1004827
- 696 24. Robertson AL, Ogryzko N V, Henry KM, et al. Identification of benzopyrone as a  
697 common structural feature in compounds with anti-inflammatory activity in a zebrafish  
698 phenotypic screen. *Dis Model Mech*. 2016;9(6):621-632. doi:10.1242/dmm.024935
- 699 25. Lauber K, Bohn E, Kröber SM, et al. Apoptotic cells induce migration of phagocytes  
700 via caspase-3-mediated release of a lipid attraction signal. *Cell*. 2003;113(6):717-730.  
701 doi:10.1016/S0092-8674(03)00422-7
- 702 26. Tyas L, Brophy VA, Pope A, Rivett AJ, Tavaré JM. Rapid caspase-3 activation during  
703 apoptosis revealed using fluorescence-resonance energy transfer. *EMBO Rep*.  
704 2000;1(3):266-270. doi:10.1093/embo-reports/kvd050
- 705 27. Pittman K, Kubes P. Damage-Associated Molecular Patterns Control Neutrophil  
706 Recruitment. *J Innate Immun*. 2013;5(4):315-323. doi:10.1159/000347132
- 707 28. de Oliveira S, Rosowski EE, Huttenlocher A. Neutrophil migration in infection and  
708 wound repair: going forward in reverse. *Nat Rev Immunol*. 2016;16(6):378-391.  
709 doi:10.1038/nri.2016.49
- 710 29. de Oliveira S, Reyes-Aldasoro CC, Candel S, Renshaw SA, Mulero V, Calado A.  
711 *Cxcl8* (IL-8) mediates neutrophil recruitment and behavior in the zebrafish

- 712 inflammatory response. *J Immunol.* 2013;190(8):4349-4359.  
713 doi:10.4049/jimmunol.1203266
- 714 30. Lämmermann T. In the eye of the neutrophil swarm--navigation signals that bring  
715 neutrophils together in inflamed and infected tissues. *J Leukoc Biol.* 2015;100(July).  
716 doi:10.1189/jlb.1MR0915-403
- 717 31. Heit B, Robbins SM, Downey CM, et al. PTEN functions to “prioritize” chemotactic  
718 cues and prevent “distraction” in migrating neutrophils. *Nat Immunol.* 2008;9(7):743-  
719 752. doi:10.1038/ni.1623
- 720 32. Heit B, Tavener S, Raharjo E, Kubes P. An intracellular signaling hierarchy  
721 determines direction of migration in opposing chemotactic gradients. *J Cell Biol.*  
722 2002;159(1):91-102. doi:10.1083/jcb.200202114
- 723 33. Stephen J, Scales HE, Benson RA, Erben D, Garside P, Brewer JM. Neutrophil  
724 swarming and extracellular trap formation play a significant role in Alum adjuvant  
725 activity. *npj Vaccines.* 2017;2(1):1. doi:10.1038/s41541-016-0001-5
- 726 34. Nüsslein-Volhard C (Christiane), Dahm R. *Zebrafish : A Practical Approach.* Oxford  
727 University Press; 2002.
- 728 35. Rougeot J, Zakrzewska A, Kanwal Z, Jansen HJ, Spaink HP, Meijer AH. RNA  
729 Sequencing of FACS-Sorted Immune Cell Populations from Zebrafish Infection  
730 Models to Identify Cell Specific Responses to Intracellular Pathogens. In: Humana  
731 Press, New York, NY; 2014:261-274. doi:10.1007/978-1-4939-1261-2\_15
- 732 36. Athanasiadis EI, Botthof JG, Andres H, Ferreira L, Lio P, Cvejic A. Single-cell RNA-  
733 sequencing uncovers transcriptional states and fate decisions in haematopoiesis. *Nat*  
734 *Commun.* 2017;8(1):2045. doi:10.1038/s41467-017-02305-6
- 735 37. Samarut É, Lissouba A, Drapeau P. A simplified method for identifying early CRISPR-  
736 induced indels in zebrafish embryos using High Resolution Melting analysis. *BMC*  
737 *Genomics.* 2016;17:547. doi:10.1186/s12864-016-2881-1
- 738 38. Parant JM, George SA, Pryor R, Wittwer CT, Yost HJ. A rapid and efficient method of  
739 genotyping zebrafish mutants. *Dev Dyn.* 2009;238(12):3168-3174.  
740 doi:10.1002/dvdy.22143
- 741 39. Pollitt EJG, Szkuta PT, Burns N, Foster SJ. Staphylococcus aureus infection  
742 dynamics. Prince A, ed. *PLOS Pathog.* 2018;14(6):e1007112.  
743 doi:10.1371/journal.ppat.1007112

744 **Supplemental Figures**

745

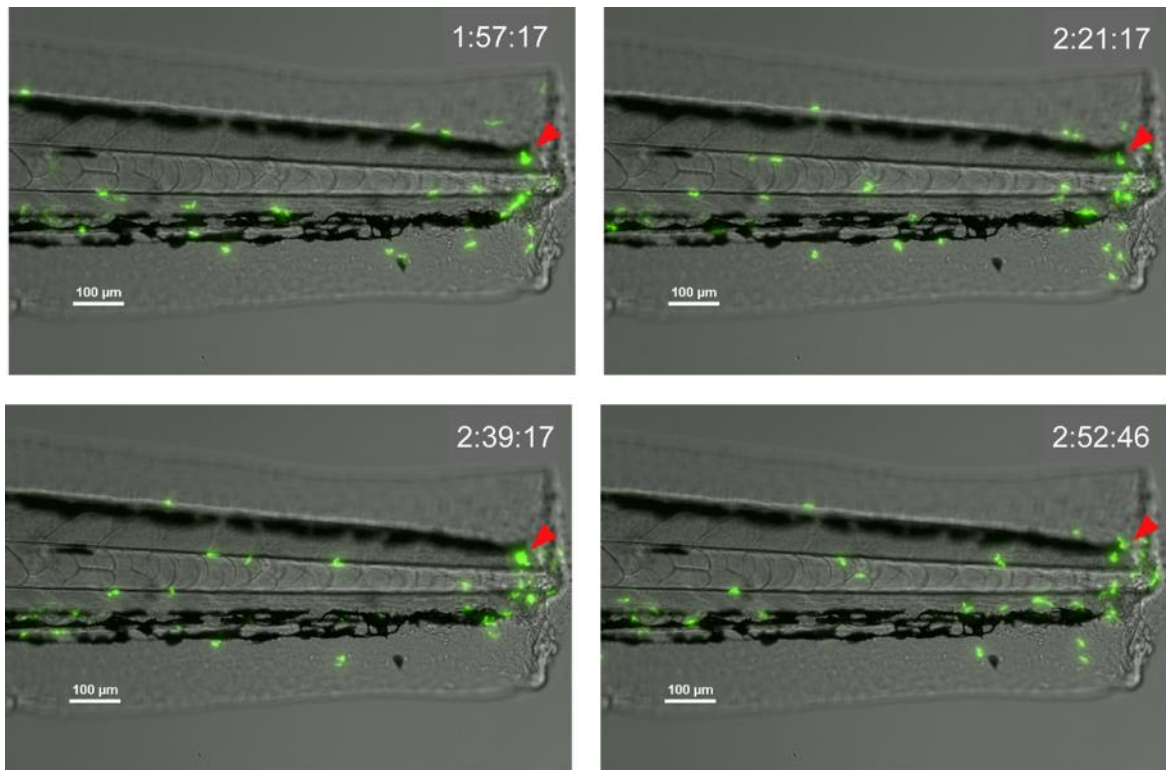


746

747 **Supplemental Figure 1. Dynamics of the neutrophil response to tissue injury**

748 Following tail-fin transection of *mpx:GFP* transgenic larvae, the number of GFP neutrophils at  
749 the site of injury were counted at 2, 4, 6, 8, 12 and 24 hours post injury. **A.** Representative  
750 images illustrating neutrophils in the tail fin region throughout the time course. **B.**  
751 Quantification of neutrophil counts at the wound site throughout the time course. Data are  
752 shown as mean  $\pm$  SEM,  $n = 53$  larvae from 3 independent experiments.

753

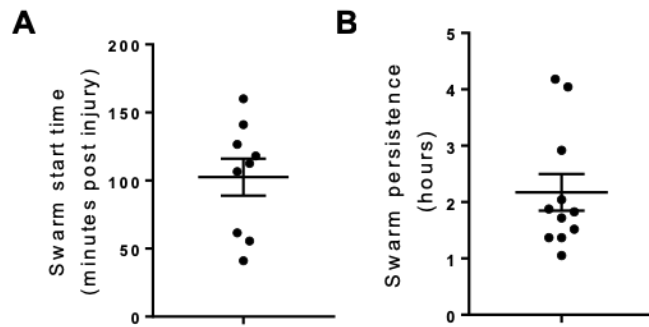


754

755 **Supplemental Figure 2. Transient neutrophil swarms are observed within the inflamed**  
756 **tail fin**

757 Time course of *mpx*:GFP transgenic zebrafish larvae following tail-fin transection illustrating  
758 short-lived (<1 hour) transient neutrophil swarming at the wound site. Phases of coordinated  
759 migration resulting in swarm formation (red arrow) were observed within the imaging period,  
760 followed by dissipation and re-formation. Time stamps shown in white (h:mm:ss) are relative  
761 to the start of imaging at 30 minutes post injury.

762

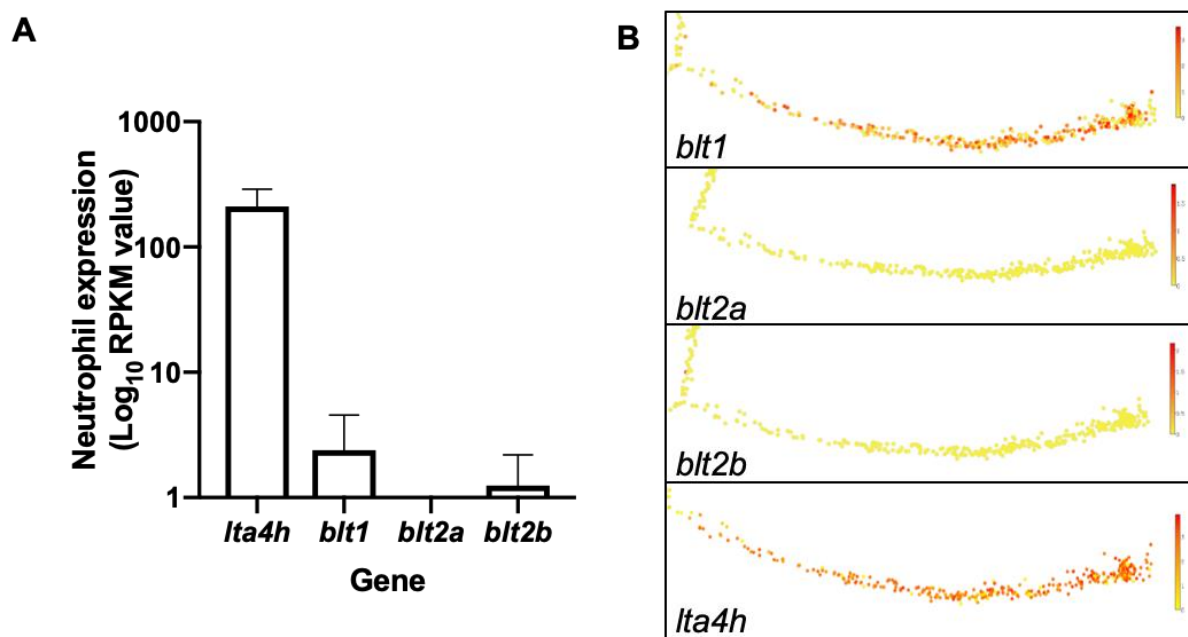


763

764 **Supplemental Figure 3. Characterisation of persistent neutrophil swarms**

765 **A.** Time (minutes post injury) in which persistent neutrophil swarms began to develop following  
766 tail-fin transection in zebrafish larvae (n=5 experimental repeats). **B.** Persistence time of  
767 neutrophil swarms measured during 5 hour imaging period (n=5 experimental repeats).

768



769

770 **Supplemental Figure 4. Expression of LTB4 signalling components in zebrafish**  
771 **neutrophils**

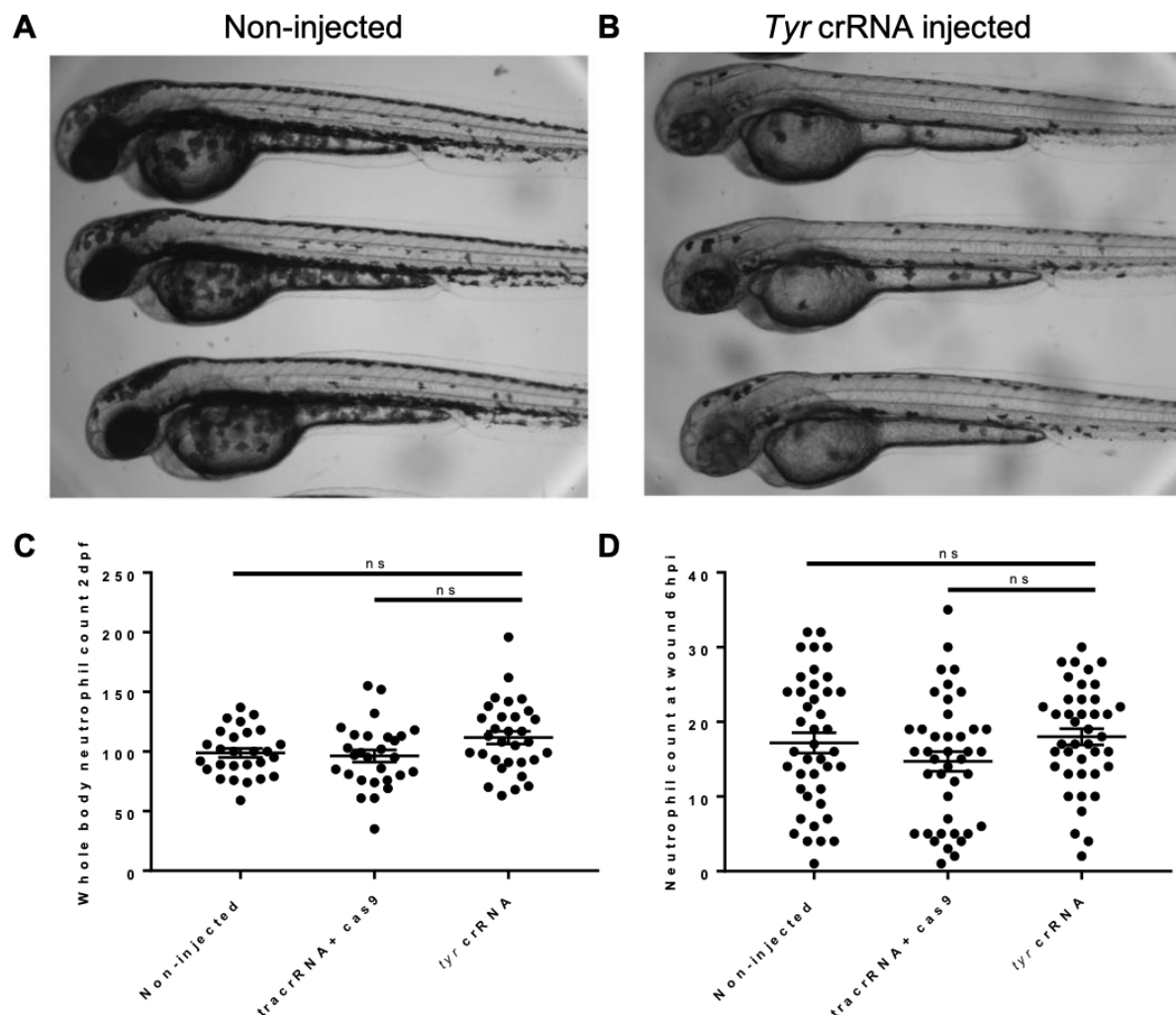
772 **A.** RNA sequencing of FACS sorted GFP positive cells from 5dpf *mpx:GFP* zebrafish larvae.  
773 RPKM values illustrate zebrafish neutrophil expression of *lta4h*, *blt1*, *blt2a* and *blt2b*. **B.**  
774 Single-cell gene expression profiles of LTB4 signalling components expressed in zebrafish  
775 neutrophils. Figure shows two-dimensional monocle plots illustrating individual neutrophil



776 expression profiles (circles) taken from FACS sorted cells from *mpx*:GFP positive transgenic  
777 larvae. Gene expression is colour coded where red is high expression and yellow is no  
778 expression. Data extracted from the Sanger BASiCz (Blood atlas of single cells in zebrafish)  
779 cloud repository.

780

781



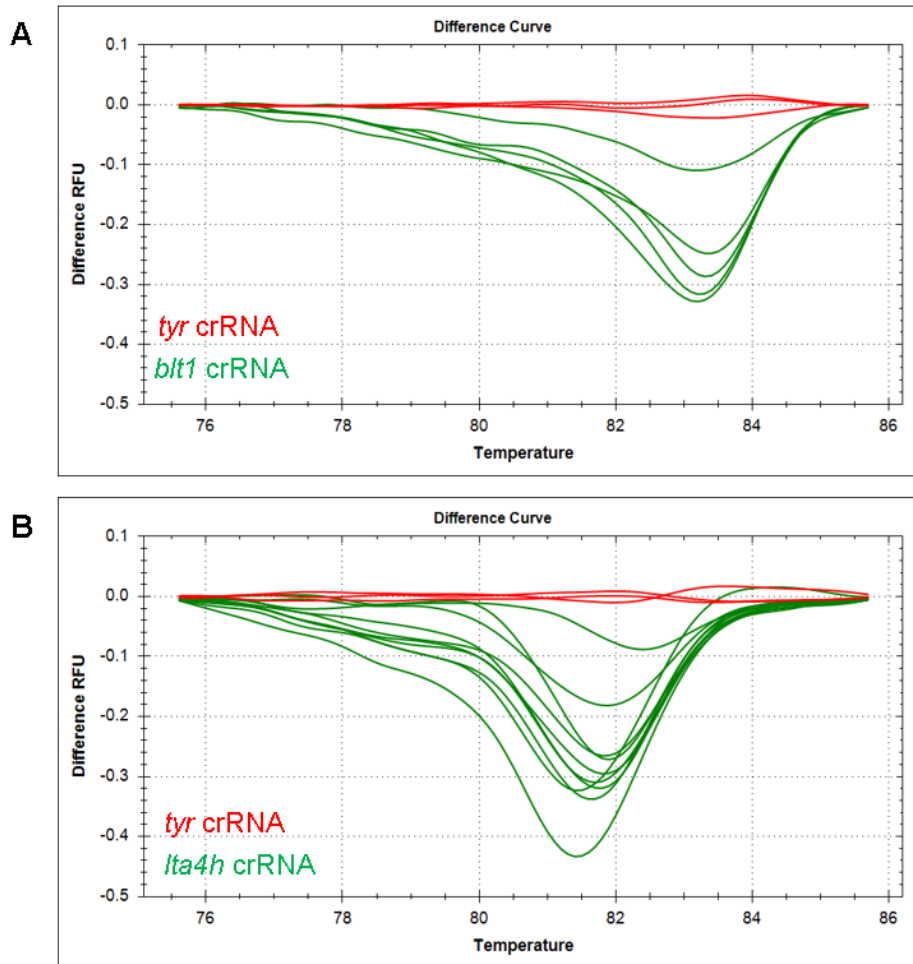
782

783 **Supplemental Figure 5. CRISPR/Cas9 knockdown of *tyrosinase* does not affect**  
784 **neutrophil function**

785 **A-B.** Representative images of 2dpf *mpx*:GFP non-injected (**A**) and tyrosinase crRNA injected  
786 (**B**) mosaic pigment phenotypes. **C.** Whole body neutrophil counts in non-injected, vehicle  
787 control tracrRNA + cas9 protein injected and *tyrosinase* crRNA injected larvae. **D.** Neutrophils  
788 recruited to the injury site at 6hpi in 2dpf non-injected, vehicle control tracrRNA + cas9 protein

789 injected and *tyrosinase* crRNA injected larvae. Error bars shown are mean  $\pm$  SEM. Groups  
790 were analysed using an ordinary one-way ANOVA and adjusted using Tukey's multi  
791 comparison test, n=30 from 3 independent experiments.

792

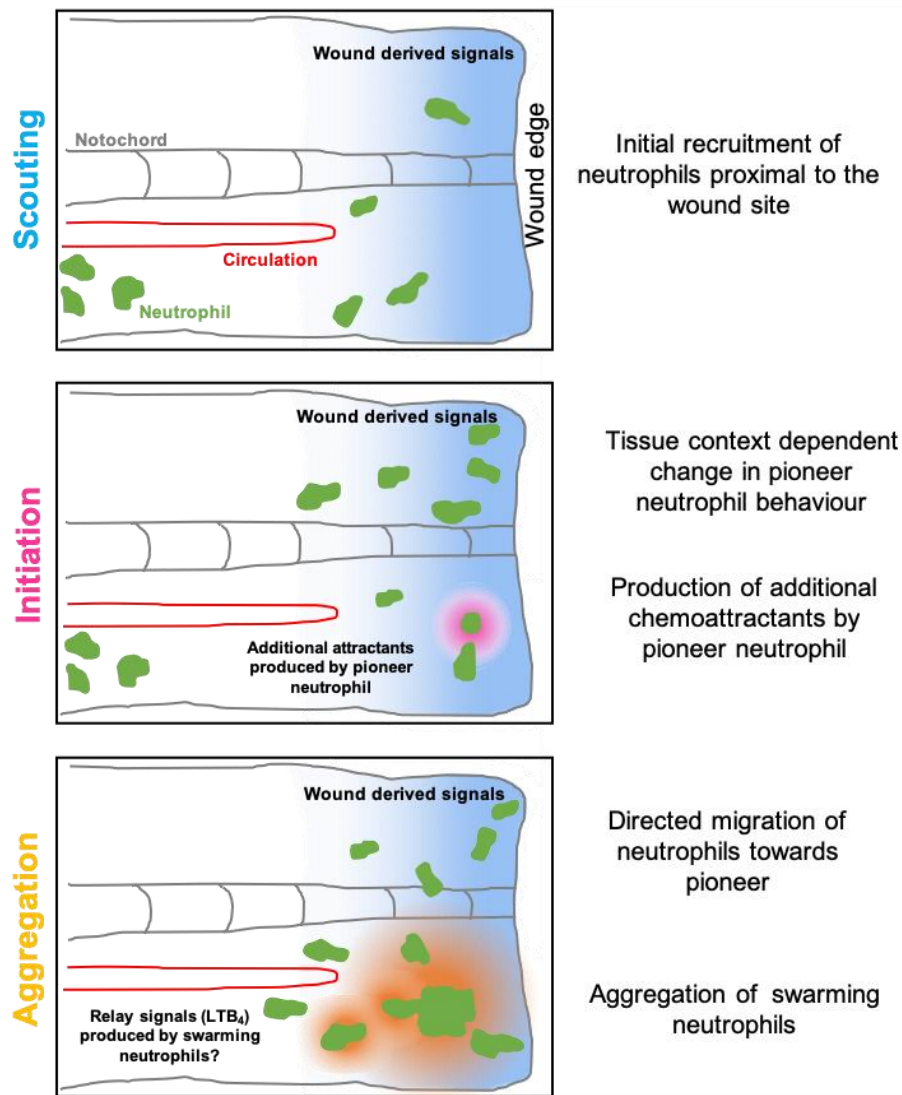


793

794 **Supplemental Figure 6. High resolution melt curve analysis for genotyping *blt1* and**  
795 ***lta4h* CRISPR knockdown**

796 Genotyping example of successful CRISPR-induced indels by high resolution melt analysis  
797 for *blt1* (A) and *lta4h* (B) injected larvae. Wild type curves (red) from three representative  
798 control *tyrosinase* larvae and shifted, irregular melt curves (green) corresponding to mosaic  
799 heteroduplex PCR fragments formed as a result of CRISPR/Cas9 mutations.

800



801

802 **Supplemental figure 7. Proposed schematic of endogenous neutrophil swarm initiation**  
803 **at sites of tissue injury**

804 Following tail fin transection neutrophils proximal to the wound site migrate towards wound-  
805 derived chemoattractants (scouting). Swarming is initiated when one pioneer neutrophil at the  
806 wound site changes behaviour and releases additional chemoattractant gradients which are  
807 responded to by a population of neutrophils (initiation), resulting in the directed migration of  
808 neutrophils to form a swarm (aggregation). The precise tissue context required for swarm  
809 initiation and the mediators released by the pioneer remain to be determined.

810

811